

Appendix S1

Satellite cell isolation and culture

Satellite cells were isolated and grown following established methods.¹ Briefly, muscle samples were digested for 30 minutes in a 37°C temperature-controlled magnetic stir-flask with 0.0025g Collagenase II (Worthington) in 5 mL DMEM (Thermo Fisher Scientific) per 1g of tissue. Mononuclear cells were isolated using a magnetic-activated cell sorting (MACS) strategy outlined in the Miltenyi MultiSort protocol for cells with the surface markers neural cell adhesion molecule 1 (NCAM1) and C-X-C motif chemokine receptor type 4 (CXCR4) (anti-NCAM1 and anti-CXCR4, both at 2.5 ng/mL, Miltenyi). In brief, the cell suspension was diluted 4x in MACS PEB buffer, pH 7.2 (Miltenyi) and filtered through a 30 um mesh strainer to obtain mononuclear cells. The cells were pelleted at 300 x g for 20 minutes at 4°C, and the supernatant was discarded. Blocking of nonspecific protein binding sites was achieved with MACS PEB buffer containing 20% bovine serum albumin (BSA; Miltenyi, San Diego, CA) for 15 minutes in the dark at 4°C. A MACS PEB buffer rinse was followed by incubation with the first antibody-conjugated microbead (NCAM1). Cells were rinsed and passed through a magnetic column to collect the NCAM1-positive fraction. The magnetic column was washed with additional MACS PEB to remove unlabeled cells. Magnetically labeled cells were flushed from the column after removal from the magnet and collected. The NCAM1-microbead was removed with a bead cleaving agent to allow for subsequent labeling of the second selection antibody (CXCR4). The cells collected in the second magnetic labeling were thus doubly positive for NCAM1 and CXCR4. This method resulted in a nearly pure satellite cell population as verified by positive PAX7 immunofluorescence signal obtained from cells cultured for 24-48 hours. Anti-PAX7 was prepared from PAX7 hybridoma cells obtained through the Developmental Studies Hybridoma Bank (DSHB; deposited by Kawakami, A.).

Validated satellite cell-derived myoblast populations were grown in proliferation medium consisting of Zenbio Skeletal Muscle Growth Medium (Zenbio) supplemented to a final concentration of 20% Qualified FBS (Thermo Fisher Scientific), 4 g/L of dextrose (Thermo Fisher Scientific), 1 ng/mL of human bFGF (PeproTech), and 1% penicillin-streptomycin (Thermo Fisher Scientific), was exchanged every other day until cells reached confluence. Upon reaching confluence, cultures were rinsed with Dulbecco's phosphate-buffered saline, pH 7.2, containing magnesium and calcium, and then medium consisting of high glucose DMEM (Thermo Fisher Scientific) supplemented with 2% horse serum (Thermo Fisher Scientific), 2% human insulin (Sigma), and 1% penicillin-streptomycin was applied to the cells for 24 hours to initiate satellite cell differentiation and myoblast fusion.² After 24 hours, cells were collected and suspended in TRIzol (Qiagen).

RNA-seq analysis

Publicly available algorithms were used to process the RNA-seq data from FASTQ files to differential gene expression. In brief, files were trimmed and filtered with *Cutadapt* (version 1.14) using the *Trim Galore* wrapper script (version 0.4.4, Babraham Bioinformatics) with a Phred-scaled quality score of ≥ 28 and a length cutoff of 30 bp. Alignment to the human genome

(hg19) was carried out using *TopHat2*³ and target feature counts were determined using *HTSeq*⁴ (version 0.9.1). Heatmaps of the DEGs were generated using *Heatmapper* with clustering based on average linkage and distance calculated as Spearman's rank correlation, which assesses the concordance between the ranks of the count values. To calculate the Spearman's rank correlation, each data value is replaced by its rank when the values are ordered. Then the correlation between the two rank vectors is calculated and these correlations are used to determine how closely samples cluster to each other with higher correlation coefficients indicating closer association in the map. Principal component analysis (PCA) data were generated in RStudio using the *stats* package⁵ (version 4.0.4) and visualized in three dimensions using the *pca3d* package⁶ (version 0.10.2).

References

1. Danoviz ME, Yablonka-Reuveni Z. Skeletal muscle satellite cells: background and methods for isolation and analysis in a primary culture system. *Methods Mol Biol* 2012;798:21-52.
2. Domenighetti AA, Mathewson MA, Pichika R, Sibley LA, Zhao L, Chambers HG, Lieber RL. Loss of myogenic potential and fusion capacity of muscle stem cells isolated from contractured muscle in children with cerebral palsy. *Am J Physiol Cell Physiol* 2018;315(2):C247-C257.
3. Langmead B, Trapnell C, Pop M, Salzberg SL. Ultrafast and memory-efficient alignment of short DNA sequences to the human genome. *Genome Biol* 2009;10(3):R25.
4. Anders S, Pyl PT, Huber W. HTSeq--a Python framework to work with high-throughput sequencing data. *Bioinformatics* 2015;31(2):166-169.
5. R Core Team (2021). R: A language and environment for statistical computing. R Foundation for Statistical Computing, Vienna, Austria. URL <https://www.R-project.org/>.
6. January Weiner (2020). *pca3d*: Three Dimensional PCA Plots. R package version 0.10.2. <https://CRAN.R-project.org/package=pca3d>.

Supplemental Table 1: List of DEGs (FDR <0.05) in spinalis muscle tissue.[†]

Upregulated					Downregulated				
Gene	logFC	logCPM	p value	FDR	Gene	logFC	logCPM	p value	FDR
RNLS	2.4	5.12	1.86E-08	1.17E-04	MDM2	-2.3	7.22	6.30E-08	1.99E-04
ABCA9-AS1	1.4	6.42	1.06E-06	1.67E-03	SHISA5	-2.1	3.72	6.12E-07	1.29E-03
CFD	2.2	3.43	2.33E-06	2.94E-03	MYO7B	-1.7	5.04	1.40E-05	9.85E-03
TPT1	1.8	7.36	9.35E-06	9.83E-03	AEBP1	-2	5.07	2.16E-05	1.10E-02
ARRDC2	2.5	5.02	1.20E-05	9.85E-03	C20orf166-AS1	-1.4	6.63	2.26E-05	1.10E-02
DMD	1.6	4.78	1.29E-05	9.85E-03	CRACR2B	-2	3.34	2.57E-05	1.16E-02
RPPH1	1.7	5.78	1.80E-05	1.10E-02	GPR39	-3.3	5.26	2.99E-05	1.26E-02
MIR548N	1.3	8.31	2.00E-05	1.10E-02	NR5A1	-3.3	5.26	3.40E-05	1.34E-02
ENO3	2.1	4.77	4.07E-05	1.35E-02	MFSD10	-2.3	3.66	4.23E-05	1.35E-02
HNRNPDL	2.3	3.07	4.19E-05	1.35E-02	GRSF1	-2	3.53	5.10E-05	1.35E-02
C1orf74	2.2	3.91	4.79E-05	1.35E-02	NCAM1-AS1	-1.7	4.35	5.32E-05	1.35E-02
LOC100506071	1.7	5.41	5.26E-05	1.35E-02	MXRA8	-1.4	6.45	5.51E-05	1.35E-02
PLCG2	1.4	6.47	5.75E-05	1.35E-02	SLC31A1	-1.6	4.33	5.75E-05	1.35E-02
LIFR	1.3	7.09	5.76E-05	1.35E-02	ZFPM1	-1.6	4.75	6.36E-05	1.38E-02
RPL13	1.4	4.04	6.21E-05	1.38E-02	PARP8	-3	4.99	6.76E-05	1.38E-02
HOXA10	2.9	3.18	6.94E-05	1.38E-02	HYLS1	-2.1	2.99	7.77E-05	1.44E-02
PDK4	2	5.54	7.02E-05	1.38E-02	ZNF629	-1.6	3.51	8.15E-05	1.45E-02
SPRTN	1.4	6.4	7.76E-05	1.44E-02	MAPT	-1.6	4.54	1.08E-04	1.83E-02
CSNK1D	2.5	5.59	8.27E-05	1.45E-02	WNK2	-2.6	3.76	1.10E-04	1.83E-02
CD59	1.9	3.08	1.17E-04	1.83E-02	CDAN1	-1.5	5	1.19E-04	1.83E-02
ACTA1	1.4	8.62	1.32E-04	1.86E-02	P2RY14	-2.6	3.66	1.19E-04	1.83E-02
HSP90AB1	1.5	6.17	1.37E-04	1.86E-02	SEBOX	-2.5	2.81	1.23E-04	1.84E-02
DYNC112	1.3	5.59	1.38E-04	1.86E-02	MIR6723	-4.6	11.99	1.38E-04	1.86E-02
MYL1	2.1	4.54	1.42E-04	1.86E-02	PRR29-AS1	-1.8	2.91	1.39E-04	1.86E-02
ARL6IP4	1.5	4.74	1.60E-04	2.02E-02	FAXDC2	-1.3	5.3	1.46E-04	1.89E-02
CKM	1.5	7.77	1.68E-04	2.08E-02	FDPSP2	-1.3	5.79	1.75E-04	2.11E-02
LINC01504	2.3	3.17	2.42E-04	2.77E-02	NRIP3	-2	3.42	1.77E-04	2.11E-02
ARRDC3-AS1	1.3	5.68	2.60E-04	2.84E-02	SPIB	-2.2	3.67	2.04E-04	2.38E-02
PLG	2	4.97	2.76E-04	2.95E-02	TRIM17	-1.4	3.8	2.54E-04	2.84E-02
UBB	1.4	4.59	2.93E-04	2.98E-02	PFN4	-1.9	2.88	2.61E-04	2.84E-02
GIGYF2	1.8	3.21	2.97E-04	2.98E-02	AKR1C2	-1.4	5.13	2.81E-04	2.95E-02
MEF2C	1.5	4.71	3.94E-04	3.64E-02	SYNGAP1	-1.9	2.56	2.95E-04	2.98E-02
ST13	1.6	3.91	4.93E-04	4.21E-02	POU5F1	-1.7	3.24	3.20E-04	3.16E-02
TXNIP	1.8	3.93	4.94E-04	4.21E-02	PTGFRN	-3	3.82	3.30E-04	3.18E-02
STAG3L4	1.4	6.99	5.06E-04	4.21E-02	LOC100506100	-2.3	2.71	3.33E-04	3.18E-02
RPL14	1.5	4.41	5.17E-04	4.21E-02	C8orf88	-2.3	3.54	3.88E-04	3.64E-02
FBLN2	2.1	3.1	5.21E-04	4.21E-02	MFAP5	-2.4	2.54	3.98E-04	3.64E-02
RHOBTB1	2.5	4.46	5.37E-04	4.29E-02	JAM2	-1.8	4.51	4.75E-04	4.21E-02
TECPR2	1.6	4.61	6.04E-04	4.56E-02	POU5F1P4	-1.3	3.95	4.90E-04	4.21E-02
MYOZ1	1.8	4.75	6.07E-04	4.56E-02	RTL1	-1.5	5.99	5.08E-04	4.21E-02
NFKBIA	2.2	2.94	6.79E-04	4.97E-02	LENG9	-1.4	4.58	5.21E-04	4.21E-02
					UEVLD	-2.2	2.66	5.66E-04	4.41E-02
					CAMTA2	-1.3	3.86	5.66E-04	4.41E-02
					PRPH2	-1.2	4.11	5.77E-04	4.44E-02
					CCDC125	-1.9	3.08	6.60E-04	4.90E-02
					TMEM208	-2.2	3.31	6.86E-04	4.97E-02

[†]logFC : log₂ of the fold change between CP cases and controls;

logCPM : log₂ of the average counts per million expressed;

FDR : false discovery rate (Benjamini-Hochberg) adjusted p-value

Supplemental Table 2: List of DEGs (FDR < 0.05) in SCDMTs.[†]

Upregulated					Downregulated				
Gene	logFC	logCPM	p value	FDR	Gene	logFC	logCPM	p value	FDR
GNAT1	3.26	5.41	3.31E-08	5.49E-05	LAMA4	-3.46	5.53	1.70E-13	1.27E-09
SEMA3F	2.44	5.17	3.23E-07	2.19E-04	CD248	-3.50	6.22	1.52E-09	5.65E-06
ADAMTS5	1.48	6.96	1.07E-06	6.12E-04	FAM216B	-5.99	6.35	2.29E-08	5.49E-05
LOC100128531	2.08	5.32	4.74E-06	2.36E-03	LTBP1	-3.26	4.36	4.65E-08	5.49E-05
PEG3-AS1	1.89	4.80	8.15E-06	3.38E-03	TPR	-2.96	7.20	4.73E-08	5.49E-05
MPEG1	2.17	4.19	9.50E-06	3.73E-03	PDGFRB	-2.08	6.36	5.15E-08	5.49E-05
HEYL	1.46	6.71	3.85E-05	8.21E-03	MYL5	-1.61	5.90	8.75E-08	8.16E-05
LOC105274304	1.14	6.73	4.70E-05	9.25E-03	IGFBP6	-2.77	4.78	1.13E-07	9.33E-05
DTX4	2.68	4.38	4.84E-05	9.25E-03	HGF	-5.19	8.28	1.72E-07	1.28E-04
TMEM51-AS1	2.47	6.81	5.79E-05	1.00E-02	OAF	-2.61	3.73	3.92E-07	2.44E-04
SIX2	1.49	4.76	8.80E-05	1.43E-02	PART1	-3.39	5.13	4.26E-06	2.27E-03
IGF2-AS	1.99	6.85	1.10E-04	1.68E-02	SPON2	-1.70	5.69	5.24E-06	2.44E-03
ATG101	1.57	5.26	1.22E-04	1.82E-02	PAPPA-AS1	-2.62	9.10	7.63E-06	3.35E-03
TMEM252	3.24	3.93	1.68E-04	2.37E-02	LYPD1	-2.38	4.88	1.48E-05	5.49E-03
MRPL23-AS1	2.70	4.57	1.83E-04	2.44E-02	MIR143HG	-2.74	3.58	1.57E-05	5.49E-03
SULF1	1.86	4.58	1.84E-04	2.44E-02	LOC101929095	-1.91	6.61	1.68E-05	5.49E-03
IRS2	1.32	5.31	2.10E-04	2.56E-02	MGST1	-2.75	4.56	1.74E-05	5.49E-03
KLF5	1.42	5.14	2.22E-04	2.67E-02	PRSS12	-1.36	6.02	1.77E-05	5.49E-03
MTHFR	2.25	6.40	2.35E-04	2.68E-02	COL6A3	-1.96	9.86	1.93E-05	5.56E-03
RHOBTB3	1.01	5.91	3.11E-04	3.41E-02	GFM1	-3.57	3.89	1.94E-05	5.56E-03
LOC101928841	1.80	5.83	3.88E-04	4.12E-02	MIR4492	-1.74	4.24	2.17E-05	6.01E-03
CRYAB	1.76	4.13	4.08E-04	4.13E-02	PRRX1	-1.50	4.93	2.29E-05	6.10E-03
LIPC	1.85	4.14	4.10E-04	4.13E-02	LBX2	-2.01	4.44	2.40E-05	6.17E-03
DPYSL4	1.17	4.92	4.66E-04	4.45E-02	LOC100996251	-1.70	6.42	2.69E-05	6.69E-03
NPTX2	2.15	4.62	5.43E-04	4.91E-02	LOC541472	-2.42	5.68	2.98E-05	7.17E-03
LOC101927497	1.35	6.54	5.48E-04	4.91E-02	KRT8	-2.52	5.01	3.12E-05	7.26E-03
ANTXR1	1.08	5.55	5.97E-04	4.98E-02	THAP10	-3.14	5.64	3.21E-05	7.26E-03
TRPT1	1.18	5.87	6.00E-04	4.98E-02	DLEU1	-1.94	7.72	3.85E-05	8.21E-03
					CLDN11	-2.47	3.76	4.41E-05	9.14E-03
					RGAG4	-1.90	4.57	4.79E-05	9.25E-03
					AKAP12	-1.63	6.19	5.03E-05	9.38E-03
					ODF3B	-1.83	3.92	5.20E-05	9.45E-03
					TMTC3	-3.19	3.20	5.74E-05	1.00E-02
					NUMB	-2.91	5.19	6.09E-05	1.03E-02
					THCAT158	-1.75	4.60	6.37E-05	1.06E-02
					CPM	-1.74	5.86	9.60E-05	1.52E-02
					PCOLCE-AS1	-1.88	10.34	1.02E-04	1.59E-02
					CSNK1D	-1.11	7.94	1.25E-04	1.83E-02
					ATG9B	-2.86	3.68	1.68E-04	2.37E-02
					ANPEP	-1.88	5.59	1.82E-04	2.44E-02
					EPB41	-2.82	5.67	1.90E-04	2.46E-02
					CACNA1C-AS1	-3.44	5.24	1.93E-04	2.46E-02
					METTL12	-1.30	4.68	1.95E-04	2.46E-02
					APOBEC4	-2.04	5.08	2.08E-04	2.56E-02
					HAS1	-1.45	4.71	2.31E-04	2.68E-02
					SPAG4	-2.62	6.62	2.37E-04	2.68E-02
					CACNA2D1	-1.98	5.35	2.37E-04	2.68E-02
					COL6A1	-1.37	11.04	2.58E-04	2.87E-02
					CAST	-1.31	7.81	3.32E-04	3.59E-02
					BRF2	-1.58	5.06	3.96E-04	4.12E-02
					LOC100288181	-3.47	7.86	3.97E-04	4.12E-02
					ITGA5	-1.22	6.22	4.16E-04	4.13E-02
					KIF26B	-1.70	4.66	4.20E-04	4.13E-02
					IGSF6	-1.54	5.23	4.66E-04	4.45E-02
					TNC	-3.07	5.84	4.73E-04	4.47E-02
					TREH	-1.78	8.09	5.14E-04	4.79E-02
					TRIM13	-1.42	8.87	5.22E-04	4.80E-02
					BAALC-AS1	-2.58	4.06	5.58E-04	4.91E-02
					RBM12B	-1.57	4.26	5.59E-04	4.91E-02
					ALDH1A3	-2.12	4.65	5.83E-04	4.98E-02
					TTC33	-2.02	3.42	5.84E-04	4.98E-02
					CDR1	-1.49	12.47	5.99E-04	4.98E-02

[†]logFC : log₂ of the fold change between CP cases and controls;

logCPM : log₂ of the average counts per million expressed;

FDR : false discovery rate (Benjamini-Hochberg) adjusted p-value

Table S3: Reactome pathway analysis in spinalis muscle (no linkers, FDR < 0.05).[†]

Pathway	Ratio	Total	DEG	p value	FDR	Genes
Toll-like Receptor Cascades(R)	0.0125	141	4	9.99E-05	2.88E-02	MEF2C,NFKBIA,UBB,PLCG2
Mitotic G2-G2/M phases(R)	0.0157	177	4	2.38E-04	3.43E-02	DYNC1I2,HSP90AB1,CSNK1D,UBB
Asparagine N-linked glycosylation(R)	0.02	226	4	5.99E-04	4.50E-02	DYNC1I2,CSNK1D,UBB,CD59
Prostate cancer(K)	0.0086	97	3	6.46E-04	4.50E-02	HSP90AB1,NFKBIA,MDM2
C-type lectin receptor signaling pathway(K)	0.0092	104	3	7.90E-04	4.50E-02	NFKBIA,PLCG2,MDM2
Striated Muscle Contraction(R)	0.0027	31	2	1.38E-03	4.82E-02	MYL1,DMD
Aurora A signaling(N)	0.0027	31	2	1.38E-03	4.82E-02	NFKBIA,MDM2
Oncogene Induced Senescence(R)	0.0029	33	2	1.56E-03	4.82E-02	UBB,MDM2
HSP90 chaperone cycle for steroid hormone receptors (SHR)(R)	0.003	34	2	1.66E-03	4.82E-02	DYNC1I2,HSP90AB1
C-type lectin receptors (CLRs)(R)	0.0123	139	3	1.81E-03	4.82E-02	NFKBIA,UBB,PLCG2
Transcriptional regulation of pluripotent stem cells(R)	0.0032	36	2	1.85E-03	4.82E-02	POU5F1,NR5A1

[†] The letter in parentheses after each pathway gene set name corresponds to the source of the pathway annotations: R – Reactome, K – KEGG, N – NCI.

Table S4: Reactome pathway analysis in SCDMTs (no linkers, FDR < 0.05).

Pathway	Ratio	Total	DEG	p value	FDR	Genes
Focal adhesion(K)	0.0169	199	7	3.97E-13	3.21E-11	PDGFRB,LAMA4,HGF,COL6A1,TNC,COL6A3,ITGA5
PI3K-Akt signaling pathway(K)	0.0301	354	7	2.24E-11	8.95E-10	PDGFRB,LAMA4,HGF,COL6A1,TNC,COL6A3,ITGA5
Beta1 integrin cell surface interactions(N)	0.0056	66	5	1.16E-10	3.12E-09	LAMA4,COL6A1,TNC,COL6A3,ITGA5
ECM-receptor interaction(K)	0.0075	88	5	4.86E-10	9.72E-09	LAMA4,COL6A1,TNC,COL6A3,ITGA5
Human papillomavirus infection(K)	0.0281	330	6	3.33E-09	5.33E-08	PDGFRB,LAMA4,COL6A1,TNC,COL6A3,ITGA5
Extracellular matrix organization(R)	0.0223	262	5	1.11E-07	1.44E-06	LAMA4,COL6A1,TNC,COL6A3,ITGA5
Urokinase-type plasminogen activator (uPA) and uPAR-mediated signaling(N)	0.0036	42	3	1.58E-06	1.69E-05	PDGFRB,HGF,ITGA5
Beta3 integrin cell surface interactions(N)	0.0037	43	3	1.69E-06	1.69E-05	PDGFRB,LAMA4,TNC
Signaling by PDGF(R)	0.0043	51	3	2.82E-06	2.53E-05	PDGFRB,COL6A1,COL6A3
Integrin signalling pathway(P)	0.0134	158	3	8.15E-05	6.52E-04	COL6A1,COL6A3,ITGA5
Syndecan-4-mediated signaling events(N)	0.0027	32	2	1.54E-04	1.08E-03	TNC,ITGA5
Signaling events mediated by TCPTP(N)	0.003	35	2	1.84E-04	1.10E-03	PDGFRB,HGF
NCAM signaling for neurite out-growth(R)	0.0046	54	2	4.36E-04	2.62E-03	COL6A1,COL6A3
MicroRNAs in cancer(K)	0.0264	310	3	5.92E-04	2.96E-03	PDGFRB,TNC,ITGA5
Melanoma(K)	0.0061	72	2	7.71E-04	3.86E-03	PDGFRB,HGF
EGFR tyrosine kinase inhibitor resistance(K)	0.0067	79	2	9.26E-04	4.63E-03	PDGFRB,HGF
Protein digestion and absorption(K)	0.0081	95	2	1.33E-03	5.33E-03	COL6A1,COL6A3

† The letter in parentheses after each pathway gene set name corresponds to the source of the pathway annotations: R – Reactome, K – KEGG, N – NCI.

Table S5: DEGs grouped by function.

Function	Muscle tissue DEGs	SCDMT DEGs
Cytoskeletal structure	MYL1, MYOZ1, DMD, ACTA1, MYO7B	EPB41, KRT8, MYL5
Extracellular structure	FBLN2, AEBP1, MFAP5, MXRA8	COL6A1, COL6A3, ITGA5, LAMA4, LTBP1, SULF1, TNC
Metabolism	ENO3, PDK4, CKM, FDPSP2, AKR1C2	ALDH1A3, APOBEC4, CPM, CSNK1D, DPYSL4, DTX4, HAS1, LIPC, MTHFR, PRSS12
Development and growth	TPT1, HOXA10, ARRDC2, NFKBIA, PLG, MEF2C, CAMTA2, POU5F1, WNK2	ADAMTS5, ANPEP, ANTXR1, CAST, CD248, CRYAB, IGSF6, KLF5, LBX2, NUMB, PRRX1
Stress/cell death/autophagy	TXNIP, ST13, TECPR2, HSP90AB1, UBB, TRIM17, SHISA5, TMEM208	ATG101, ATG9B
Gene regulation	ABCA9-AS1, ARRDC3-AS1, MIR548N, C20orf166-AS1, NCAM1-AS1, PRR29-AS1, MIR6723	BAALC-AS1, CACNA1C-AS1, DLEU1, IGF2-AS, MIR143HG, MIR4492, MRPL23-AS1, PAPPB-AS1, PART1, PCOLCE-AS1, PEG3-AS1, THCAT158, TMEM51-AS1
Receptor composition	LENG9, NRIP3, P2RY14, PTGFRN, NR5A1, GPR39, LIFR	IRS2, PDGFRB
Signaling	CSNK1D, RHOBTB1, PLCG2, PFN4	CSNK1D, RHOBTB3, SEMA3F, SIX2

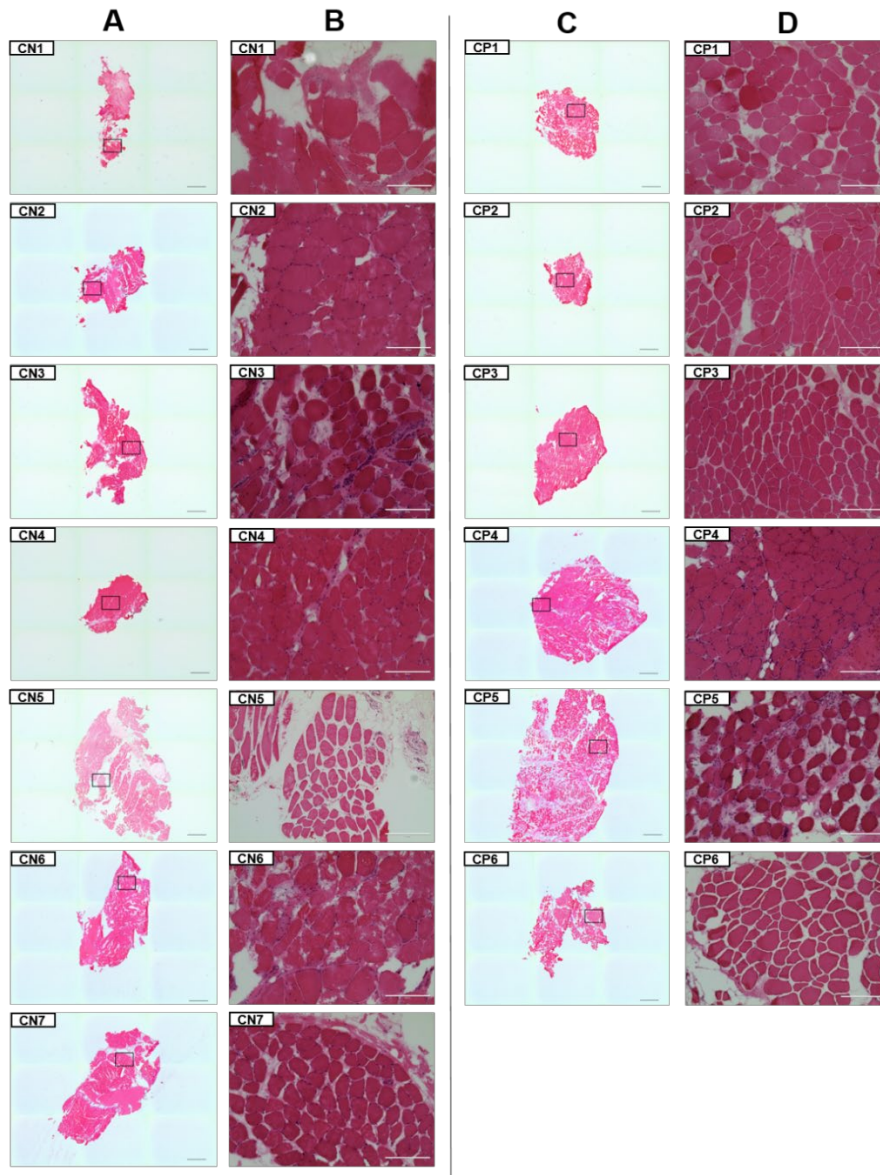


Figure S1: Hematoxylin and eosin images of skeletal muscle samples. For samples used for the skeletal muscle tissue analysis, 8-10 μ m sections of each biopsy were stained with hematoxylin and eosin to assure that samples comprised predominantly muscle fibers. Tiled images of the entire tissue section were taken at 4x (A: comparison individual, C: CP; scale bars = 1000 μ m) and zoomed images of the areas in rectangles were taken at 20x (B: comparison individual, D: CP; scale bars = 200 μ m) on an EVOS FL Auto Imaging System. Variability in fiber size/shape and the extent of extracellular matrix was observed in samples from both groups and was not considered exclusionary.

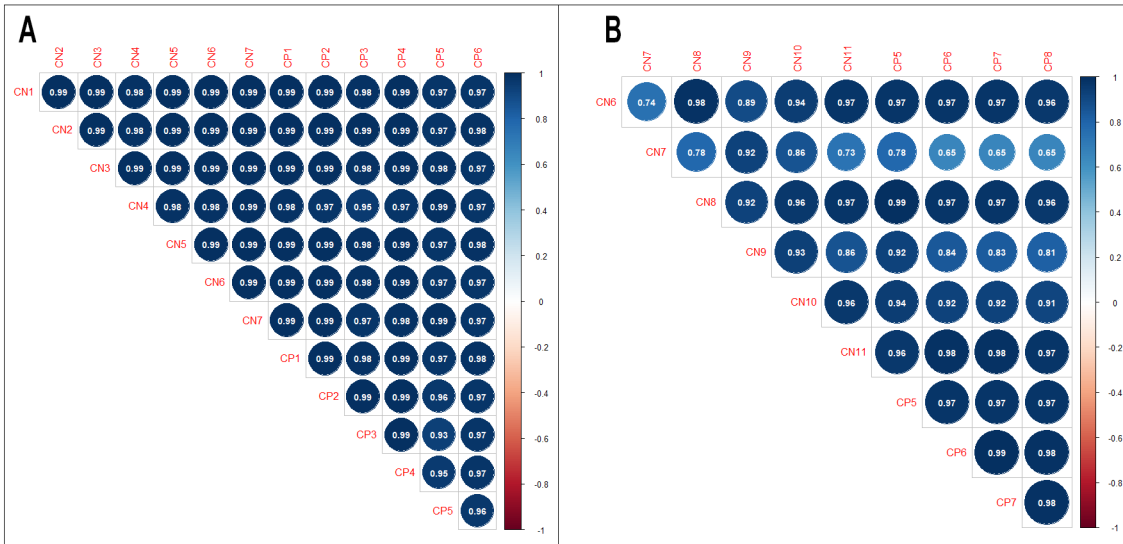


Figure S2: Correlation of RNA-seq count data per participant. Pearson's correlation coefficients between RNAseq counts from pairs of participants are represented in a correlogram for muscle tissue (A) and SCDMTs (B). Positive correlations are displayed in blue. Color histogram shows the range of Pearson r values, and the relative size of each circle is proportional to its correlation coefficient.

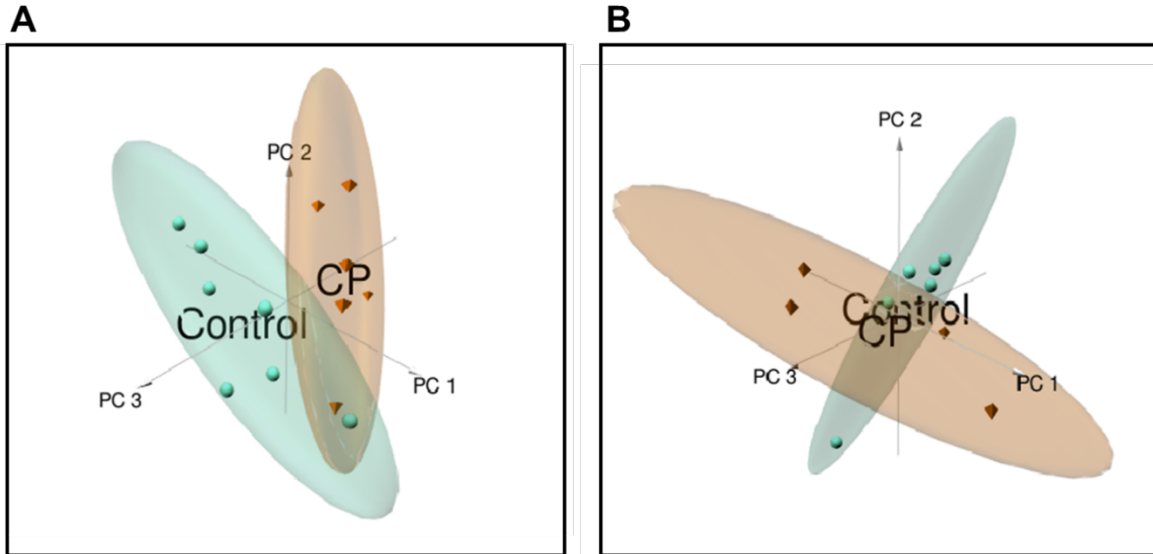


Figure S3: Principal component analysis to identify discriminating gene expression patterns between CP and non-CP cohorts. For both muscle tissue (A) and SCDMTs (B), the first three component axes were plotted to locate the individual participant points. Each point represents the similarity position of a participant based on all expressed genes ($n = 6308$ for muscle tissue and 7459 for SCDMTs). The first three principal components (PC) explained 47.1% of the variance for muscle (PC1 = 20.5%, PC2 = 17.3%, PC3 = 9.3%) and 62.6% of the variance for SCDMTs (PC1 = 30.0%, PC2 = 21.3%, PC3 = 11.3%). Comparison: green points, CP: orange points. Ellipses represent 90% confidence intervals.

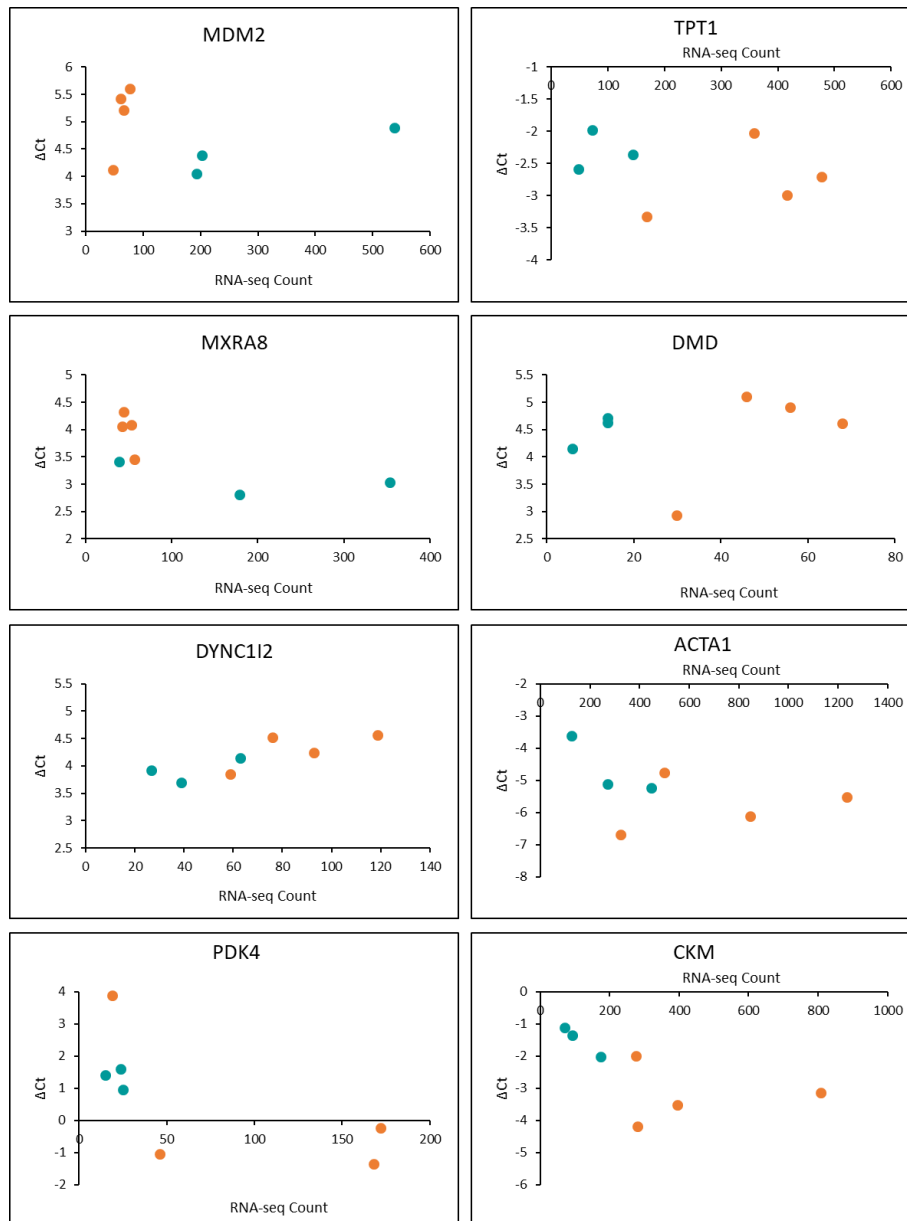


Figure S4: qPCR validation of RNA-seq data in skeletal muscle. qPCR validation was performed on the top 3 most significant genes from three different functional categories: *MDM2*, *TPT1*, and *MXRA8* for signaling, *DMD*, *DYNC1|2*, and *ACTA1* for structural, and *PDK4*, *CKM*, and *AKRIC* for metabolic. *AKRIC* was excluded from analysis because it did not amplify. RNA-seq counts were plotted against Δ Ct values (threshold cycle for the target gene minus threshold cycle for the *B2M* housekeeping gene) with an inverse relationship between RNA-seq count and Δ Ct expected. Each point represents a sample with comparison in green and CP in orange.

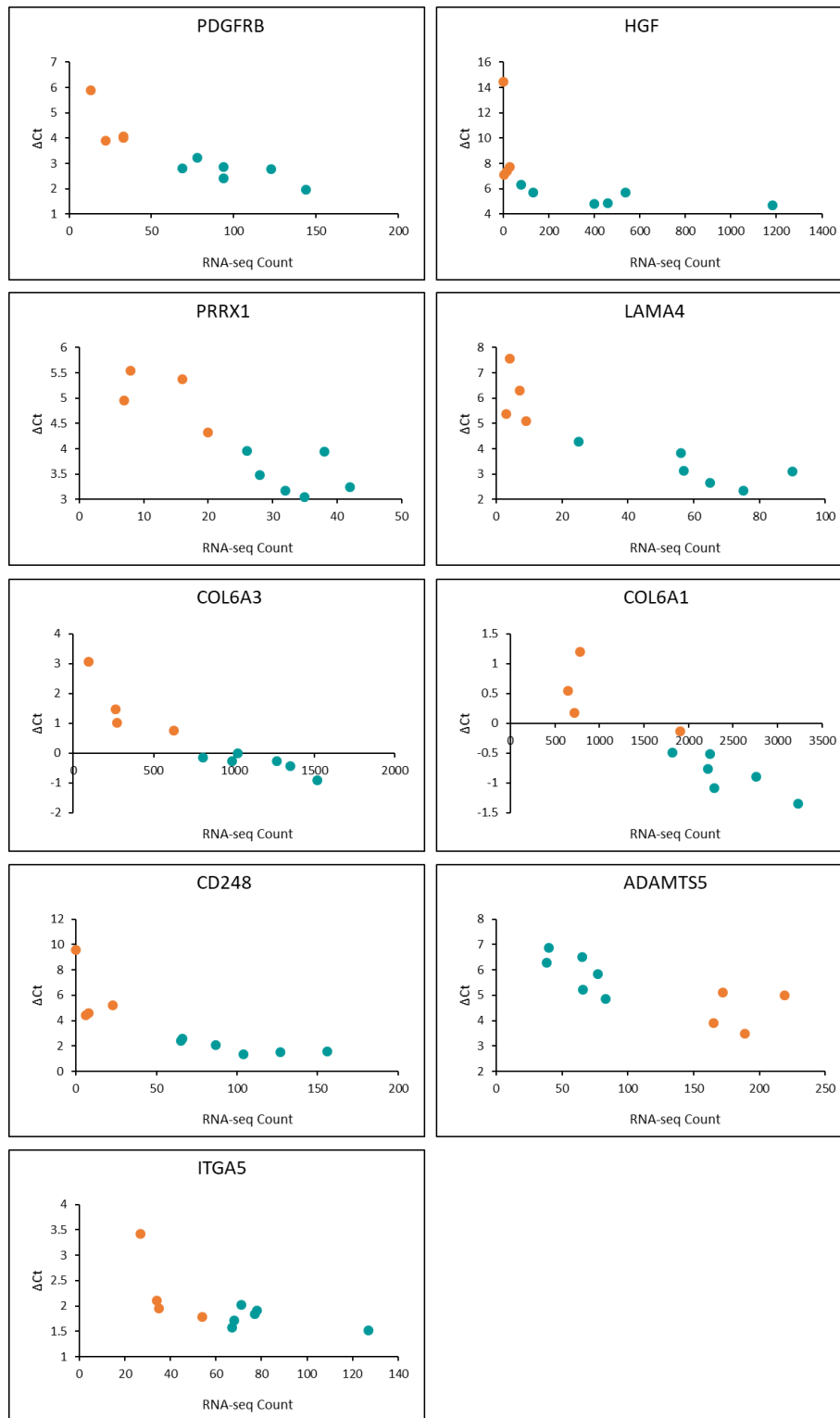


Figure S5: qPCR validation of RNA-seq data in SCDMTs. qPCR validation was performed on the top 3 most significant genes from three different functional categories: *PDGFRB*, *HGF*, and *PRRX1* for signaling, *LAMA4*, *COL6A3*, and *COL6A1* for ECM, and *CD248*, *ADAMTS5*, and *ITGA5* for ECM-binding. RNA-seq counts were plotted against ΔCt values (threshold cycle for the target gene minus threshold cycle for the *B2M* housekeeping

gene) with an inverse relationship between RNA-seq count and ΔC_t expected. Each point represents a sample with comparison in green and CP in orange.